Full Paper
doi.org/10.1002/chem.202003478
Chemistry Europe
European Chemical Societies Publishing

Dynamics

Configurational and Constitutional Dynamics of Enamine Molecular Switches

Yansong Ren,[a] Oleksandr Kravchenko,[a] and Olof Ramström*[a, b, c]

Abstract: Dual configurational and constitutional dynamics in systems based on enamine molecular switches has been systematically studied. pH-responsive moieties, such as 2-pyridyl and 2-quinolinyl units, were required on the „stator" part, also providing enamine stability through intramolecular hydrogen-bonding (IMHB) effects. Upon protonation or deprotonation, forward and backward switching could be rapidly achieved. Extension of the stator π-system in the 2-quinolinyl derivative provided a higher *E*-isomeric equilibrium ratio under neutral conditions, pointing to a means to achieve quantitative forward/backward isomerization processes. The „rotor" part of the enamine switches exhibited constitutional exchange ability with primary amines. Interestingly, considerably higher exchange rates were observed with amines containing ester groups, indicating potential stabilization of the transition state through IMHB. Acids, particularly Bi^{III}, were found to efficiently catalyze the constitutional dynamic processes. In contrast, the enamine and the formed dynamic enamine system showed excellent stability under basic conditions. This coupled configurational and constitutional dynamics expands the scope of dynamic C–C and C–N bonds and potentiates further studies and applications in the fields of molecular machinery and systems chemistry.

Introduction

Coined by Wittig in 1927,[1] enamines have been considered structural analogs of enols, containing a carbon-carbon double bond conjugated with an amino substituent. The electron-donating nitrogen increases the nucleophilicity of the olefin part, which in turn renders it a valuable activated intermediate in many organic transformations.[2] The integration of the *en*- and *amine*-moieties also equips the enamine derivatives with an attractive dual dynamic feature: configurational dynamics—controlled by physical or chemical factors, such as thermal-, photo- or pH- activated *E*/*Z*-isomerization; and constitutional dynamics—exchange of the amine or carbonyl component through an amine-enamine exchange reaction.[3]

Constitutional exchange using dynamic interactions/reactions of non-covalent or covalent nature can lead to the formation of controllable and responsive systems.[4] When integrated with configurational switching, dynamic covalent chemistry based on reactions, such as imine and hydrazone formation/exchange as well as thiol-disulfide exchange, has also been applied for the construction of molecular switches and machines.[5] However, examples exploiting C=C double bonds in dynamic chemistry or molecular machinery are relatively limited in comparison with the well-documented use of C=N double bonds (imines/hydrazones). To this end, we previously reported the first enamine-based molecular switch (Scheme 1),[3a] in which the forward and backward configurational rotation around the C=C double bond could be precisely operated, for example, by consecutive additions of acid and base. The enamine functionality also enabled a double dynamic regime where the configurational switching could be regu-

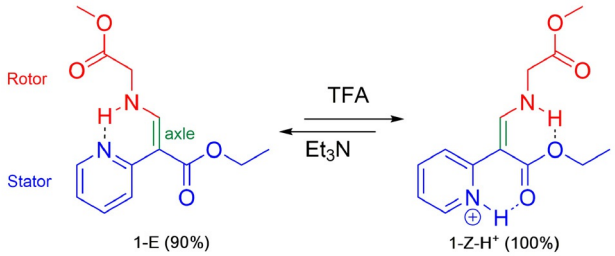

Scheme 1. pH-controlled enamine molecular switch **1**.

[a] *Dr. Y. Ren, O. Kravchenko, Prof. Dr. O. Ramström*
Department of Chemistry
KTH—Royal Institute of Technology
Teknikringen 36, 10044 Stockholm (Sweden)

[b] *Prof. Dr. O. Ramström*
Department of Chemistry
University of Massachusetts Lowell
One University Ave., Lowell, MA 01854 (USA)
E-mail: olof_ramstrom@uml.edu

[c] *Prof. Dr. O. Ramström*
Department of Chemistry and Biomedical Sciences
Linnaeus University, 39182 Kalmar (Sweden)

Supporting information and the ORCID identification number(s) for the author(s) of this article can be found under: https://doi.org/10.1002/chem.202003478.

Part of a Special Issue celebrating the 1000th Issue of Chemistry—A European Journal.

lated in conjunction with constitutional enamine exchange on the amine rotor part. The exchange process could also be turned on and off through regulation of the pH.

This coupled dynamic switching and exchange allows for novel possibilities to control the properties of complex molecular systems, potentially resulting in emergent properties and enabling new approaches towards advanced information storage and processing.[6] However, for such dual dynamic entities, several challenges need to be addressed. For a configurational switch, the isomerization efficiency is of primary concern, where quantitative conversion to either configuration is desired. On the other hand, for constitutional chemistry applications, critical features include the robustness of the system, the reaction scope, and the performance of the dynamic exchange. These challenges have been addressed in the present study, where we describe the enamine switching properties in relation to modular variations of the rotor and stator, and the efficiency of the rotor exchange process with respect to structural-, catalytic- and pH-effects.

Results and Discussion

Configurational enamine switch

Diversity of rotors

Intramolecular hydrogen bonding (IMHB) has been shown in many cases to stabilize enamines in their less stable configuration.[7]

By conjugating the enamine moiety to a π-system or adding/inducing charges, the overall H-bonding can furthermore be stabilized through resonance-assisted hydrogen bonding (RAHB) or charge-assisted hydrogen bonding (CAHB) effects.[8] In the present case, conjugating the enamine in molecular switch **1** with an ester group, and introducing a 2-pyridyl moiety next to the C=C axle, provide stabilizing effects of either configuration. Since the pyridyl group is a stronger hydrogen bonding acceptor than the ester group towards the enamine NH, the *E*-form is favored under neutral/basic conditions (Scheme 2, left). Furthermore, the pyridyl moiety furnishes the molecule with responsiveness towards acidic conditions. Protonation of the pyridine eliminates the pyridyl N···H–N H-bonding and promotes the rotor to switch to the thermodynamically more stable *Z*-form, which can be potentially stabilized by RAHB and CAHB effects (Scheme 2, right).

Enamine **1** exhibited good switching reversibility under alternating acid/base-conditions (Figure S1 in Supporting Information). Predominantly in the *E*-form (91%) in CD_3CN, addition of 2.0 equiv of Et_3N did not change the *E*/*Z* ratio. However, addition of 5.0 equiv of TFA to the basic solution led to complete switching to the *Z*-form, and subsequent addition of Et_3N (7.0 equiv) restored the original *E*/*Z* ratio. This process could be repeated at least four cycles without significant loss of switching efficiency. This alternating switching process can potentially be managed using photoacids.[9]

In order to test the influence of the rotor part, a series of primary amine rotors bearing various functionalities were readily assembled with the ethyl 2-pyridylacetate stator by a one-step condensation reaction (Scheme 3). As can be seen from the ^{1}H-NMR spectra, the *E*-configuration of compounds **2**–**14** dominated the isomeric equilibrium under neutral conditions, similarly to molecular switch **1**. The enamine NH-signals of both the *E*- (10.83–14.43 ppm) and the *Z*- (8.70–11.87 ppm) isomers

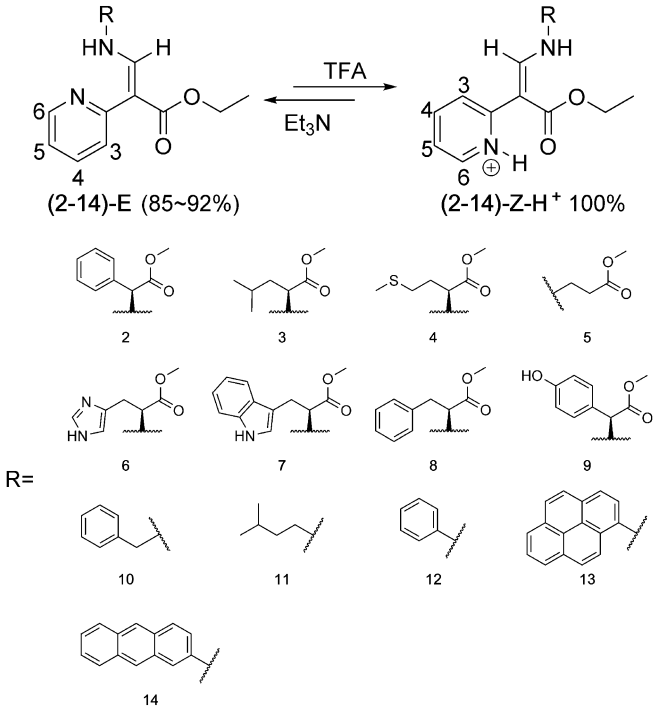

Scheme 3. Enamine-based switch system with different rotor structures. Stable isomers in solution and their protonated products are shown.

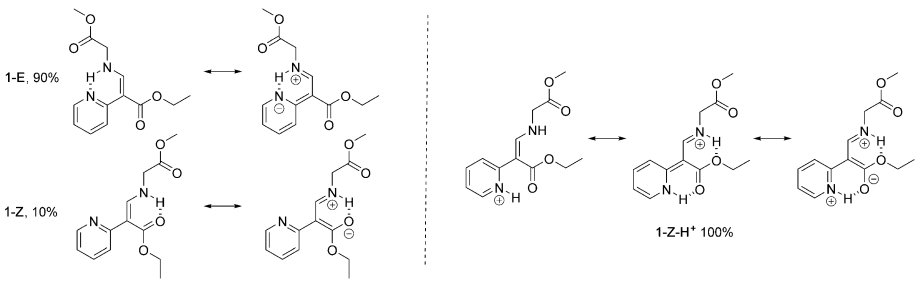

Scheme 2. RAHB effect in **1-E** and **1-Z** (left); RAHB and CAHB effects in **1-Z-H$^+$** (right).

resonated at a lower field beyond the aromatic region, indicating an RAHB effect with the pyridyl or the ester group.[10] Interestingly, the *E*-isomers containing aliphatic amine rotors (**2**–**11**) showed an 85–89% equilibrium ratio, whereas the ratio of the aromatic amines (**12**–**14**) increased to 90–92%. Compounds **11** and **13** exhibited the lowest (85%) and highest (92%) degrees of *E*-isomer, respectively. This indicates the ability of aromatic rotors to form a larger π-system conjugated with the pyridyl moiety in the *E*-isomers than in the *Z*-forms, resulting in greater π-delocalization of the enamine NH-group via an RAHB effect; thus the energy gaps of the *E*/*Z*-isomers are enlarged.

With the decrease of the rotor amines' pK_{aH} values, the ^{1}H-NMR signals of the NH-protons generally shifted to the downfield region (Figures S2–4). For compounds **10**–**14**, the positions of the enamine NH-signals for both the *E*- and the *Z*-isomers demonstrated a clear linear relationship with the pK_{aH}-values of their rotor primary amines. However, for compounds **1**–**9**, whose rotors were derived from amino acid methyl esters, the shifts of the NH signals tended to deviate from the linear dependency to a highfield region. This effect is likely accounted for by the reduction of the σ co-planarity degree between the amino acid carbonyl group and the amino hydrogen after being assembled on the switches. The crystal structure of isomer **1-E** exhibited a 56.6° dihedral angle between the Py-C=C-NH and the NH-CH_2-$COOCH_3$ planes, resulting in a weak C=O···HN IMHB. Compounds **2** and **5** showed less deviation from the linear relationship than other α-amino acid ester derivatives (**3**–**4**, **6**–**8**). The ^{1}H-NMR spectra for the α-amino acid ester derivatives revealed that the $^2J_{NH\ CHR}$-constants in compounds **3**–**4** and **6**–**8** were approximately 8.8 Hz, whereas this number dropped to 7.4 Hz in compounds **2** and **5**. This implies an increase in the σ co-planarity between the amino acid carbonyl group and the amino hydrogen due to the smaller dihedral angles.

The performance of the enamine switches **2**–**14** upon protonation/deprotonation was next examined. The results were similar to compound **1-E** (Figures S5–14) and the addition of a slight amount of TFA to solutions of compounds **(2–14)-E** in $CDCl_3$ immediately decreased the relative amount of the *E*-isomers. The addition of 2.0 equivalents of TFA completely induced the forward switching, except for compound **6-E**, where 3.0 equivalents of TFA were required in order to additionally protonate the imidazole ring. To these acidic solutions containing only *Z*-H^+-isomers, the addition of equimolar or slightly excess amounts of Et_3N resulted in backward switching and rapidly restored the original equilibrium. All of the enamines showed very good stability during the switching process, including compounds **10**–**14** that lack extra stabilization of the enamine NH from the methyl ester side chains.

Besides the *E*/*Z* ratio changes, the ^{1}H-NMR spectroscopy study showed that the *E*-isomers' NH-signals became progressively broader in response to the increasing TFA content along with decreasing spin-spin coupling constants of the pyridyl-H6- and enamine CH-protons, whereas the NH-signals of the *Z*-isomers remained sharp and generally shifted to the downfield region. Moreover, correlations between the olefin CH- and the pyridyl-H3 protons (compare Scheme 3) existed in 2D-NOESY-NMR spectra of the *Z*-H^+-isomers. These observations show that the addition of TFA not only led to the protonation of the pyridine moiety but also to exchange with the *E*-NH proton, possibly facilitating the enamine ⇄ imine tautomerization process through the rotation of the iminium group via a C–C single bond and the formation of thermodynamically favored *Z*-H^+-isomers.[11]

Importance of stator

The stator of enamine **1-E**, ethyl 2-pyridylacetate, was replaced by different aryl systems. A phenyl group was first tested, where both compounds **Ph-1-Z** (41%) and **Ph-1-E** (15%) could be isolated from the reaction mixture as pure isomers. Isomer **Ph-1-E** in a CD_3CN solution slowly isomerized to isomer **Ph-1-Z** with a rate of $(8.92 \pm 0.27) \times 10^{-10}\,M^{-1}s^{-1}$ at rt, which was almost two times faster than the rate of $Z \rightarrow E$ isomerization ($(4.55 \pm 0.11) \times 10^{-10}\,M^{-1}s^{-1}$). However, the *E*/*Z* ratio immediately changed to 27:73 after the addition of 1.0 equiv TFA to either isomer in CD_3CN, accompanied by broadening of the *E*/*Z*-NH proton signals (Scheme 4). The acid induced a large acceleration of the isomerization rates indicating a tautomerization mechanism for the $E \rightleftarrows Z$ interconversion. A full conversion could not be achieved even when the amount of TFA was increased to 10 equiv, which resulted in an equilibrium of approximately 33:67 (**Ph-1-E**:**Ph-1-Z**). This ratio did not change significantly after the subsequent addition of an equimolar amount of Et_3N (Figure S15). The 4-pyridyl stator (**4Py-1**) exhibited a 10:90 *E*/*Z* ratio in CD_3CN, the low *E*-configuration ratio reflected by the lack of an IMHB between the enamine-NH and the pyridine ring. Complete switching to enamine **4Py-1-Z-H$^+$** was observed after protonation (Scheme 4, Figure S16).

An analog of enamine **1-E** was prepared using a 2-quinolinyl-group as part of the stator. Enamine **Qui-1-E** possessed a high *E*/*Z* isomeric ratio (97:3) in CD_3CN under neutral conditions, which subsequently equilibrated to 95:5 after a few hours. The characteristic ^{1}H-NMR signals of the enamine-NH were located at 11.81 ppm (*E*) and 8.75 ppm (*Z*) (Figure 1a) matching those of switch **1-E**. Noticeably, an approximate 1 ppm difference to the downfield region from the NH-signal of isomer **Qui-1-E** could be observed compared to that of isomer **1-E** located at 10.80 ppm (Figure 1c), whereas this chemical shift difference was only 0.14 ppm for their corresponding *Z*-isomers (Figure 1a and 1c). These differences indicate that the enamine **Qui-1-E** exhibits a more pronounced RAHB effect on the N···HN H-bonding than that of enamine **1-E** because of the extension of a larger π-system. Since this type of RAHB effect is much less pronounced in isomer **Qui-1-Z**, the extension of the conjugated system results in a larger energy gap between isomers **Qui-1** *E* and *Z* isomers and elevated the *E*-isomer to a thermodynamic distribution of 95%.

In order to completely convert enamine **Qui-1-E** into its *Z*-H^+ isomer, 2.8 equivalents of TFA were required (Figure 1b). This amount is higher than that required to switch enamine **1-E** to **1-Z-H$^+$** (2.0 equiv, Figure 1d), which is accounted for by the lower basicity of the quinoline over the pyridine moiety. Upon protonation, the proton-signals of **Qui-1-Z-H$^+$** in the aro-

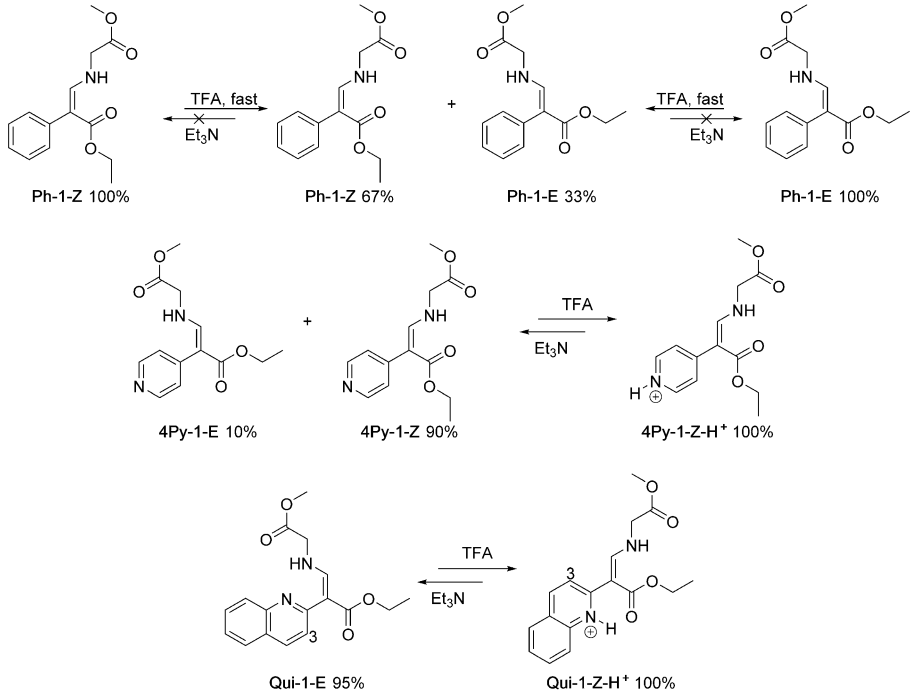

Scheme 4. Enamine-based switch systems with different stators. The stable isomer(s) in solution and the protonated products are shown.

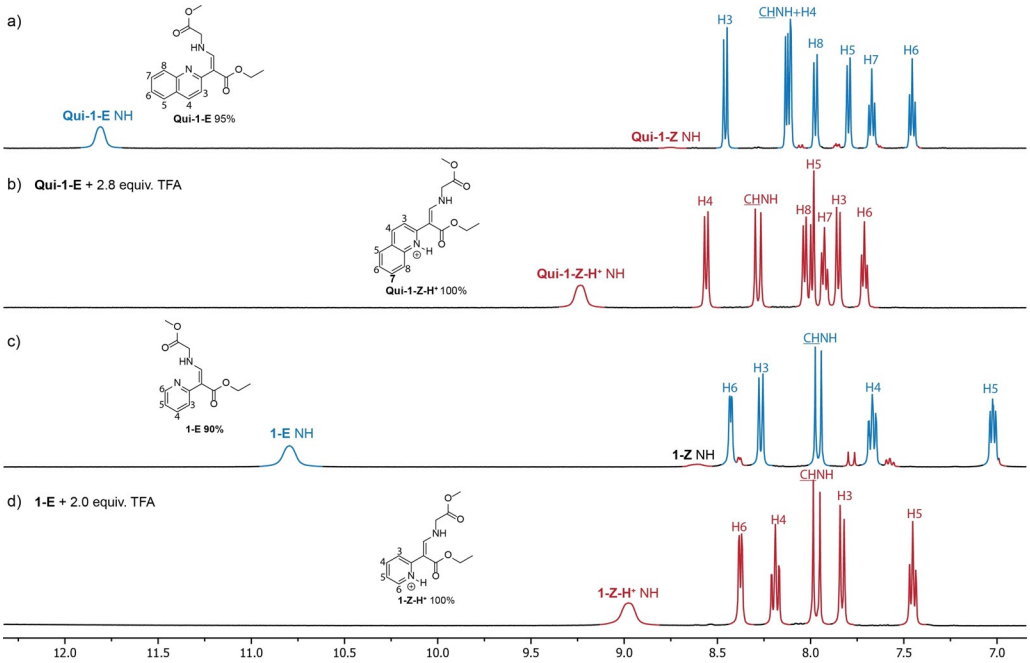

Figure 1. ^{1}H-NMR spectra (500 MHz) illustrating the two configurations of enamine switches **Qui-1** and **1** in CD_3CN at 23 °C. a) Equilibrium distribution between isomers **Qui-1-E** (95%, blue) and **Qui-1-Z** (5%, red); b) complete forward switching of **Qui-1-E**: addition of 2.8 equiv TFA to a) leading to isomer **Qui-1-Z-H$^+$**; c) Equilibrium distribution between isomers **1-E** (90%, blue) and **1-Z** (10%, red); d) complete forward switch of **1-E**: addition of 2.0 equiv TFA to c) leading to isomer **1-Z-H$^+$**.

matic region shifted to the downfield region except for proton H3. In the 2D-NOESY-NMR spectra, a correlation between H3 and C=C–H could be observed only after protonation (compare Scheme 4, Figure S19), demonstrating that the protonated quinolinyl unit most likely was oriented towards the carbonyl ester face in the switched configuration. The complete backward switching process (Figure S17) could be easily accomplished by the addition of 3.0 equiv of Et_3N to the protonated isomer **Qui-1-Z-H$^+$** (2.8 equiv TFA) in CD_3CN.

Theoretical calculations of the switching process

Isomerization of enamine **1-E** to enamine **1-Z** under neutral conditions was first considered. Quantum chemical calculations were performed using the Gaussian 09 package,[12] with the B3LYP functional[13] and the 6-31G(d,p) basis set.[14] It is worth noting that the configuration of the *E*-isomer ester group could be neglected in the calculations due to the low energy barriers for rotation about the C–C bond located between the enamine C=C bond and the ester group (9.4 kcal mol^{-1}). Similarly, the configurations of the pyridyl moiety (6.8 kcal mol^{-1}) and the ester group (12.4 kcal mol^{-1}) in the *Z*-isomer were not essential. In order to enable rotation around the enamine C=C bond in isomer **1-E**, the bond order of the enamine carbon-carbon bond should become close to unity. This can be realized via a transition state with significant charge transfer from the enamine to the pyridine ring or via tautomerization to the imine (Scheme 5).

The calculation results show that the zwitterionic transition state **TS-Rot1** exhibits a high energy barrier of 32.5 kcal mol^{-1}, which cannot be easily realized at rt. There are two possible tautomers of enamine **1-E**: imines **1-ImA1** and **1-ImB1**. Imine **1-ImA1** is less stable (+15.2 kcal mol^{-1}) due to the loss of conjugation between the pyridine, imine, and the ester groups. On the other hand, all three moieties can rotate freely without forming zwitterionic intermediates. Therefore, imine **1-ImA1** can easily change conformation to imine **1-ImA2** that can potentially tautomerize into enamine **1-Z**. Such a switching route requires imine-enamine tautomerization, where acidic or basic catalysis is typically applied because a direct [1,3]-hydride shift is forbidden for geometrical reasons. Given that the concentration was too low for the enamine to act as an internal proton acceptor, it is possible that trace moisture from the solvent could participate in the tautomerization; however, the calculated transition energy for this process was 35.8 kcal mol^{-1}, which is not consistent with our experimental results. Imine **1-ImB1** can be easily formed via simple proton transfer in a 6-membered transition state, where the pyridine moiety acts as a proton acceptor through an RAHB effect. In this case, the barrier of rotation around the C–C bond in state **TS-Rot3** was 25.1 kcal mol^{-1} (Figure 2), which yields a highly conjugated imine **1-ImB2**, which then tautomerizes to enamine **1-Z**. Unlike other stimuli-induced proton transfer effects, the tautomerization in these enamine switches under neutral conditions is an equilibrium process through a resonance-assisted H-bonding effect. Such tautomerization was also found in an azo-hydrazone tautomerization process.[15]

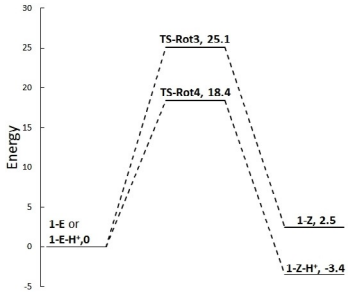

Figure 2. Energy level diagrams for enamine switching process under neutral and acidic conditions.

In an acidic environment, however, the complete switching process is likely to proceed through another mechanism (Scheme 6). The pyridine nitrogen can easily accept the proton, disrupting the intramolecular hydrogen bond and facilitating the enamine/iminium resonance. This results in a lower rotation barrier of state **TS-Rot4** (18.4 kcal mol^{-1} vs. 25.1 kcal mol^{-1}). The protonated species are also additionally stabilized (−3.4 kcal mol^{-1}) by alternative hydrogen bonding between the pyridinium and carbonyl groups in enamine **1-Z-H$^+$**.

In view of the above, we rationalize that differentiation of the rotors has a minor influence on the stability of the enam-

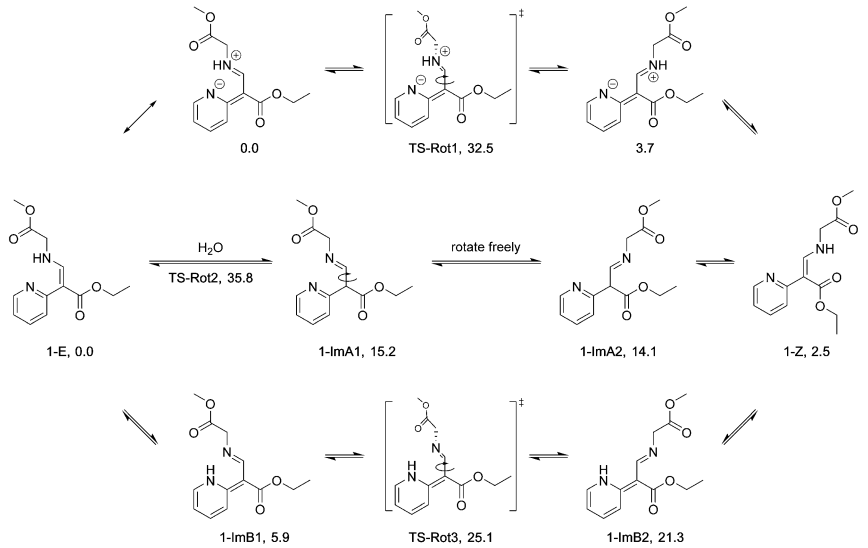

Scheme 5. Plausible routes for enamine switching under neutral conditions; calculated Gibbs energies (kcal mol^{-1}) shown.

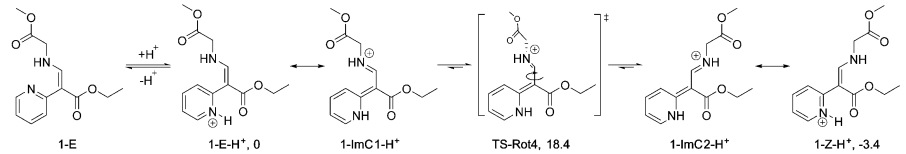

Scheme 6. Enamine switching assisted by addition of acid; calculated Gibbs energies (kcal mol^{-1}) shown.

ines and the performance of the switching processes; besides, aromatic rotors exhibit higher initial *E*-isomeric ratios. In order to construct efficient pH-responsive enamine molecular switches, the stator part thus becomes crucial to provide the driving force and stability: i) a responsive moiety should be installed to give a complete isomer (**1**–**14**, **4Py-1**, **Qui-1**) upon protonation; ii) the nitrogen atom in these heterocycles (**1**–**14**, **Qui-1**) located adjacent to the C=C-axle provides a stable IMHB in the *E*-configuration and also renders a stable hydrogen bond with the ester group after protonation. The extension of the stator to a quinolinyl-group supplies a significant increment of the *E*-isomeric equilibrium distribution to 95% under neutral conditions via an RAHB effect, which, with further modifications, holds the potential to achieve a complete *E* (100%) ⇄ *Z* (100%) isomerization switch.

Constitutional enamine exchange

Structure-activity relationship of competing rotors

The dynamic features concerning the constitutional exchange characteristics of the switch rotor part were next systematically investigated. The tested competing rotors ranged from primary aromatic amines to aliphatic amines, including amino acid derivatives bearing a variety of functional groups. Compound **1-E** was first chosen as system component together with different amine reactants in order to generate dynamic systems containing four isomeric enamine species and two amines as illustrated in Scheme 7. Enamine **1-E** and the amines were mixed in 1:1 ratios (0.03 mmol) in CD_3CN (0.5 mL) in NMR tubes, and the experiments were implemented at 60 °C. The exchange process was followed by ^{1}H-NMR spectroscopy and the obtained results are presented in Table 1, Entries 1–12.

At 60 °C, all tested amines (**A2–A13**) were capable of exchange with glycine methyl ester, the rotor of compound **1-E**, leading to the formation of dynamic enamine systems containing new enamine switches. The enamines showed generally good stability during the exchange processes, and no decom-

Table 1. Enamine exchange between enamine switches and primary amines[a]

Entry	Enamine/Amine	k_f [M^{-1} h^{-1}][b]	Selectivity[c]	K_{eq}[d]
1	**1-E/A2**	2.01	1.27	1.62
2	**1-E/A3**	3.03	1.56	2.45
3	**1-E/A4**	2.58	2.03	4.12
4	**1-E/A5**	0.97	0.61	0.38
5	**1-E/A6**	0.10	0.1	0.01
6	**1-E/A7**	0.55	0.45	0.2
7	**1-E/A8**	2.03	2.03	4.12
8	**1-E/A9**	5.08	0.67	0.44
9	**1-E/A10**	0.052	2.23	4.95
10	**1-E/A11**	0.091	1.63	2.66
11	**1-E/A12**	0.011	n.d.[e]	n.d.[e]
12	**1-E/A13**	0.030	n.d.[e]	n.d.[e]
13	**11-E/A1**	0.56	0.82	0.67
14	**4-E/A9**	4.27	0.79	0.62
15	**9-E/A4**	3.13	1.22	1.49
16	**11-E/A4**	1.09	1.33	1.76
17	**4-E/A11**	0.075	0.85	0.73
18	**10-E/A11**	0.07	n.d.[e]	n.d.[e]
19	**11-E/A10**	0.04	n.d.[e]	n.d.[e]

[a] Enamine (0.03 mmol), amine (0.03 mmol) in CD_3CN (0.5 mL), 60 ± 1 °C, monitored by following changes of the most separated enamine signals in ^{1}H-NMR spectra at 23 °C, data were collected as the average of two individual experiments. [b] Calculated by nonlinear regression analysis towards standard reaction model (see Supporting Information). [c] Ratio of [Enamine exchanged]/[Enamine original] at equilibrium. [d] Ratio of [Enamine exchanged]^2/(1−[Enamine exchanged]^2) at equilibrium. [e] Not determined due to long reaction time.

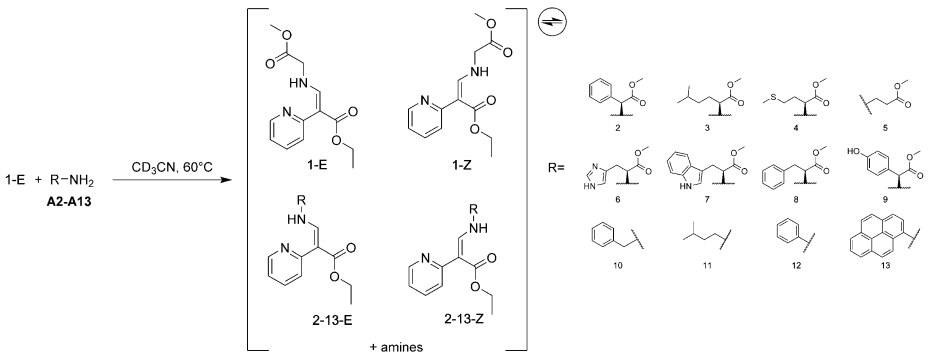

Scheme 7. Dynamic enamine system formation between enamine **1-E** and amines **A2-A13** in CD_3CN at 60 °C.

position was observed within several days under the tested conditions. It was noticed that amine **A9** displayed the highest exchange rates (5.08 $M^{-1}h^{-1}$) with enamine **1-E**, which is more than 55-fold higher than the most basic amine **A11** (0.091 $M^{-1}h^{-1}$) and ca. 460-fold faster than aromatic amine **A12** (0.011 $M^{-1}h^{-1}$). Moreover, amines derived from amino acids generally exhibited higher rates than other amines. It is clear that the aromatic amines (**A12, A13**) demonstrated the lowest rates because of their weaker nucleophilicities; however, this is not the most important factor that affects the reaction rates among aliphatic amines.

For instance, the reaction rate of amine **A3** was approximately 30 times higher than that of amine **A11** despite showing almost three orders of magnitude weaker basicity,[16] due to the electron-withdrawing methyl ester in amine **A3**. Similar results could also be recorded in the group of amines **A2/A10**. These unusual results indicate that the ester groups in the amino acid derivatives (e.g., **A2**, **A3**) play a more pronounced role in facilitating the equilibria process than the corresponding nucleophilicities of the amino groups (e.g., **A10**, **A11**),[3b,17] directing us to more thoroughly investigate the constitutional exchange process, especially the aspect of the structural effect of competing amine rotors.

Four sets of enamine/amine pairs were subsequently employed to generate dynamic enamine systems containing 0, 1, or 2 amino acid-derived amines by double-entry-point analysis under the same conditions (Scheme 8),[18] where the results are presented in Table 1, entries 13–19. The same equilibrium ratios, within the limits of the experimental error, were reached in each group, denoting the thermodynamic control in the dynamic enamine exchange process. Interestingly, pairs **10-E/A11** and **11-E/A10** showed very low rates during the equilibration process (0.07 $M^{-1}h^{-1}$ and 0.04 $M^{-1}h^{-1}$, respectively), in which no amino acid-derived amines participated. The kinetics remained slow (less than 0.01 $M^{-1}h^{-1}$) when amine **A11** was allowed to react with enamines **1-E/4-E**; however, the rate increased approximately 6-fold for glycine amino methyl ester (**A1**), and 13-fold for methionine amino methyl ester (**A4**), in reactions with enamine **11-E**. The acceleration turned more conspicuous, reaching up to 100-fold in the set of **4-E/A9** and **9-E/A4**, where both the rotor and the competitor contained ester groups. These results imply that the ester groups in the amino acid-derived amines most likely promote the exchange process by stabilizing the transition states through IMHBs. This, in turn, can facilitate the proton transfer process.[19] The ester groups in the enamines probably also take part in this process further reducing the activation energy because of the better proton affinity to the C=O moiety in comparison with the nitrogen atom.[8b,d]

In addition, a significant influence of the nature of the solvents on the reaction rates was observed (Table 2). Toluene-d_8 significantly retarded the equilibrium process between enamine **1-E** and amine **A2** compared with CD_3CN, indicating that the rate-determining step (RDS) goes through a polar TS. More interestingly, the reaction in CD_3OD showed a slower progress than in CD_3CN, excluding the possibility of the solvent acting as a proton shuttle;[20] [D_6]DMSO unexpectedly slowed down the reaction to the level of other non-amino acid-derived amines, which suggests that the strongly coordinating [D_6]DMSO diminishes the IMHB stabilization between the amino proton and the ester in TS by intermolecular hydrogen bonding.[21]

As demonstrated, the presence of pyridine and ester moieties adjacent to the enamine switch axle enabled tautomerization to form imine/iminium ion intermediates, thereby facilitating the switching process. This possibility of the imino-form co-existing with the enamine moiety also makes the switches susceptible to exchange with amines.[18,22] Thus, the enamine-amine exchange process would likely occur via the more studied transimination procedure (Scheme 9).[23] The addition of primary amines to the enamine-imine tautomeric mixture results in proton transfer in transition state **TS1**. The results sug-

Table 2. Enamine exchange between enamine **1-E** and amine **A2**[a]

Entry	solvent	k_f [$M^{-1}h^{-1}$][b]	Selectivity[c]	K_{eq}[d]
1	CD_3CN	2.01	1.22	1.49
2	CD_3OD	0.32	1.17	1.38
3	[D_6]DMSO	0.047	n.d.[e]	n.d.[e]
4	Toluene-d_8	0.07	n.d.[e]	n.d.[e]

[a] Enamine **1-E** (0.03 mmol), amine **A2** (0.03 mmol) in corresponding solvent (0.5 mL) at 60 ± 1 °C, monitored by following changes of the most separated enamine ^{1}H-NMR signals at 23 °C. [b] Calculated by nonlinear regression analysis towards standard reaction model (see Supporting Information). [c] Ratio of [Enamine **2**]/[Enamine **1**] at equilibrium. [d] Ratio of [Enamine **2**]^2/(1−[Enamine **2**]^2) at equilibrium. [e] Not determined due to long reaction time.

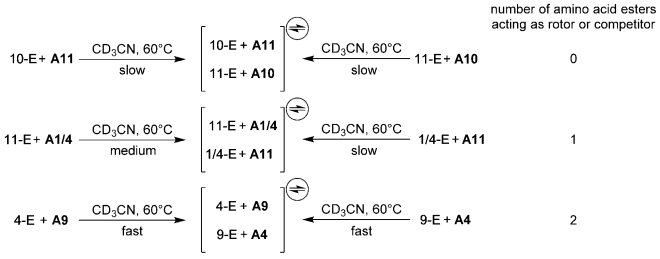

Scheme 8. Dynamic enamine system generation from two-entry-point of four sets of substrates in CD_3CN (0.5 mL) at 60 °C; relative kinetic rates (cf. Table 1) shown for comparison.

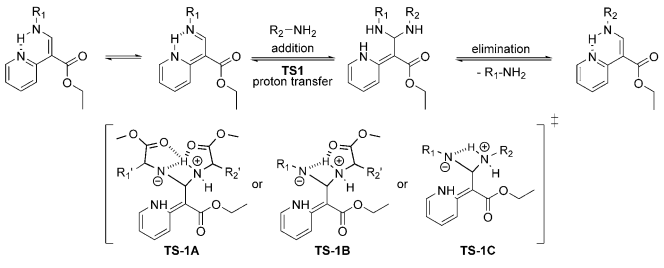

Scheme 9. General representation of the addition/elimination steps in the enamine exchange process. The plausible transition states of proton transfer processes from different starting enamine/imine combinations are illustrated.

gest that the transfer occurs between two amino groups through a 4-membered cyclic structure due to the favored polar feature, forming a transient aminal intermediate. This, followed by elimination, generates a new dynamic enamine system.

The ester groups in amino acid-derived amines likely assist in reducing the **TS** energy through an IMHB in the proton transfer step (**TS-1A**, **TS-1B**), and an even lower **TS** activation energy can be achieved when the other enamine ester group enhances the stabilization effect. Basically, towards enamine **1-E**, the k_f increases with increasing pK_a of the amines containing ester groups (Table 1, **A2** ~ **A8** < **A4** < **A3** < **A9**). A relatively low reaction rate (0.1 $M^{-1}h^{-1}$ and 0.55 $M^{-1}h^{-1}$) for amines **A6/A7** (Table 1, entries 5,6) implies that heterocycles interfere with the IMHB between the ester and amino proton most likely in the elimination step. Besides, the β-alanine methyl ester (**A5**) exhibited a moderate reaction rate considering its higher pK_a value than glycine methyl ester, which is a sign of the steric effect interfering with the double stabilization in transition states **TS1A** or **TS2A** due to a larger six-membered IMHB in this case.

In the enamine/amine exchange process, the experimental K_{eq} values were generally biased towards the enamine incorporating the more basic amine in the cases involving no or one amino acid ester (Table 1, entries 9–13, 15–19), which is similar to transimination processes.[11c,17,24] However, no clear conclusion could be drawn for the exchange process of both enamine and amine-containing amino acid esters.

Additive effects

We recently found that Brønsted and Lewis acids could efficiently catalyze the enamine exchange with secondary amines.[3b] $Sc(OTf)_3$ and $Bi(OTf)_3$ were able to accelerate the exchange processes more than 300-fold in certain cases. Such catalytic effects were also investigated in other C-*N*-type bond exchange processes, for example, transimination and hydrazone exchange.[6,17] This acidic activation occurs mainly by providing protons to avert any negative charge accumulation on the electrophile or by the polarization of the imine bond with metal ions to aid the nucleophilic attack.[23] This acceleration behavior was next studied with the present enamine systems, and the effects of acids on the enamine-amine exchange were evaluated between enamine **1-E** and primary amine **A2** in CD_3CN at 60 °C. The progress was followed by ^{1}H-NMR spectroscopy and the results are presented in Table 3 and Figure 3.

First, a series of acids including $Bi(OTf)_3$, $Sc(OTf)_3$, $Zn(OTf)_2$, $Cu(OTf)_2$ and TFA were tested separately with a loading of 5 mol%. The reaction with Bi^{III} displayed the highest rate, showing an approximate five-fold increase reaching 9.36 $M^{-1}h^{-1}$(Table 3, entry 2). Other Lewis acids, $Sc(OTf)_3$ and $Zn(OTf)_2$, also exhibited good catalytic effects (Table 3, entries 3,4). The reaction with $Cu(OTf)_2$ started smoothly; however, decomposition/byproducts became more noticeable before the equilibrium was reached. In contrast, 5 mol% addition of the Brønsted acid TFA only showed a small rate enhancement (Table 3, entry 6).

Table 3. Enamine exchange between enamine **1-E** and amine **A2** with acidic additives[a]

Entry	Additive	Loading amount	k_f [$M^{-1}h^{-1}$][b]	Acceleration[c]	Selectivity[d]	K_{eq}[e]
1	None	-	2.01	1	1.27	1.62
2	$Bi(OTf)_3$	5 mol%	9.36	4.66	1.08	1.17
3	$Sc(OTf)_3$	5 mol%	6.69	3.33	1.70	2.90
4	$Zn(OTf)_2$	5 mol%	7.37	3.67	1.22	1.49
5	$Cu(OTf)_2$	5 mol%	6.51	3.24	n.d.[f]	n.d.[f]
6	TFA	5 mol%	2.34	1.17	1.33	1.76
7	$Bi(OTf)_3$	2 mol%	4.58	2.28	1.17	1.38
8	$Bi(OTf)_3$	10 mol%	18.41	9.17	1.00	1.00
9	TFA	20 mol%	5.903	2.94	0.69	0.48
10	TFA	50 mol%	13.37	6.66	0.96	0.92
11	TFA	100 mol%	20.35	10.13	1.5	2.25
12	TFA	350 mol%	0.87	0.45	1.27	1.62

[a] Enamine **1-E** (0.03 mmol), amine **A2** (0.03 mmol) in CD_3CN (0.5 mL), 60 ± 1 °C, monitored by following changes of enamine signals in ^{1}H-NMR at 23 °C, data were collected as the average of two individual experiments. [b] Calculated by nonlinear regression analysis towards standard reaction model (cf. Supporting Information). [c] $k_f/k_{f,uncat}$. [d] Ratio of [Enamine **2**]/[Enamine **1**] at equilibrium. [e] Ratio of [Enamine **2**]^2/(1−[Enamine **2**]^2) at equilibrium. [f] Equilibrium was not reached due to side reactions.

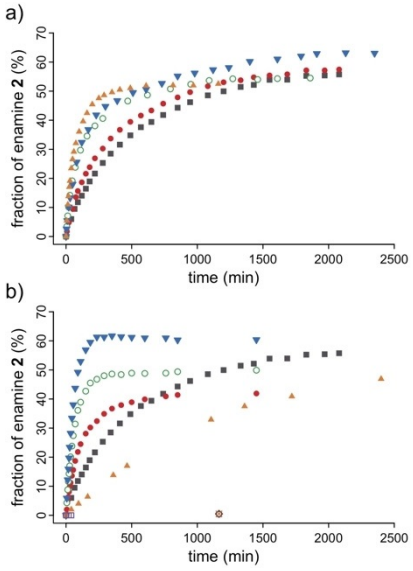

Figure 3. Enamine exchange process between enamine **1-E** (0.03 mmol) and amine **A2** (0.03 mmol) in CD_3CN (0.5 mL) at 60 ± 1 °C affected by a) addition of 5 mol% (●) TFA, (○) $Zn(OTf)_2$, (▼) $Sc(OTf)_3$, (▲)$Bi(OTf)_3$; b) addition of specific equivalents TFA (●) 0.2, (▲) 0.5, (▼) 1.0, (□) 3.5 and Et_3N (○) 0.5, (×) 1.0, (◇) 2.0. Control experiment (■) indicated in both cases. Total formation of enamine **2** (*E* + *Z*/*Z*-H^+) determined by ^{1}H-NMR spectroscopy at 23 °C.

The effects of the Bi^{III}-loading were then studied on the model reaction. After the addition of $Bi(OTf)_3$ to the pre-mixed enamine **1** and amine **A2** in CD_3CN, the ^{1}H-NMR spectra clearly displayed broadened enamine *E*/*Z*-NH signals with increased loading, indicating coordinating effects with the metal ions. Additionally, the equilibrium ratio of isomer **1-Z** increased from 10% (no catalyst) to 25% (10 mol% Bi^{III}) with its signals slightly

shifted to the downfield region. Similar spectra were also recorded in the cases of Zn^{II}-, Cu^{II}- and Sc^{III}-addition, which demonstrated that Lewis-acidic metal ions were able to catalyze the switching by coordination. Moreover, the free amine NH_2 signals shifted downfield due to the coordination effect with the metal ions.

The coordination effect between the amino groups in the enamine/amine and the Bi^{III} ion is able to assist the nucleophilic attack as well as lowering the energy barrier of the proton transfer process. A linear relationship of the k_f with the Bi^{III}-loading (0–10 mol%) was observed, suggesting a first order dependence on the catalyst (Table 3, entries 1,2,7,8, Figure S20). Thermodynamically, the fraction of enamine **2** in the equilibrated dynamic system gradually decreased from 56% to 50% as the loading of Bi^{III} was increased to 10 mol%.

The intrinsic excellent stability of the enamine molecular switches towards a large excess of TFA, as described earlier, allows for catalysis of the exchange process of system **1-E/A8** by addition of TFA up to ca. one equiv, whereas the reverse effect resulted from the addition of Et_3N or higher amounts of acid. The effects of the H^+-addition were also followed in the model transenamination process. A proportional acceleration rate with the acid loading was observed up to 1.0 equiv (Figure S21), resulting in a 10-fold increase as 1.0 equiv of TFA was applied, while the addition of excess acid (3.5 equiv) slowed down the exchange process to 0.87 $M^{-1}h^{-1}$. On the other hand, the addition of Et_3N (0.5–2.0 equiv) inhibited this dynamic process completely, showing less than 1% conversion after approximately 20 h without degradation.

The catalytic performance of Bi^{III} was then evaluated for other substrates (Table 4). A 5 mol% loading presented a minimum 2-fold acceleration compared with the corresponding uncatalyzed reactions shown in Table 1. Interestingly, the addition of Bi^{III} exhibited considerable acceleration in the cases with relatively slow rates in Table 1. Especially for **1-E/A12**-system, a 36-fold acceleration enabled the exchange process to occur smoothly with aromatic amines. Similar to the model reaction (**1-E/A2**), with the addition of metal ion, the equilibrium fraction of newly formed enamine also decreased slightly.

Additionally, the TFA effects were investigated in the exchange process of enamine **1-E** with aliphatic and aromatic amines (Table S1–3). An optimal amount of acid could accelerate the dynamic process, however, the acceleration proved highly related to the basicity of the amines. Similarly to the model reaction, the TFA effect on the exchange reaction **1-E/A9** resulted in acceleration when 0.2 to 1.0 equivalents were applied, while inhibiting the process with 2.5 equivalents. Towards enamine **1-E**, the accelerating effect of the exchange with amine **A5** was insignificant and the inhibitory effect took place after the addition of 0.5 equivalents of TFA. However, for aromatic amine **A13**, the addition of 0.2 to 1.0 equivalents of TFA showed a noticeable acceleration (up to 77-fold), excess amounts of TFA (2.5 equiv) still gave a 73-fold enhancement likely because of the lower basicity of the aromatic amine.

Table 4. Enamine exchange between enamine switches and primary amines with loading of 5 mol% $Bi(OTf)_3$ [a]

Entry	Enamine/Amine	k_f [$M^{-1}h^{-1}$][b]	Acceleration[c]	Selectivity[d]	K_{eq}[e]
1	**1-E/A3**	6.65	2.2	1.33	1.76
2	**1-E/A4**	6.27	2.4	1.38	1.91
3	**1-E/A6**	1.85	19.1	0.12	0.02
4	**1-E/A7**	6.27	11.4	0.59	0.34
5	**1-E/A8**	7.31	3.6	1.78	3.16
6	**1-E/A10**	1.17	22.5	1.04	1.08
7	**1-E/A11**	0.31	3.4	1.63	2.66
8	**1-E/A12**	0.40	36.0	1.08	1.17
9	**11-E/A1**	2.82	5.0	0.72	0.52

[a] Enamine (0.03 mmol), amine (0.03 mmol) and $Bi(OTf)_3$ 5 mol% in CD_3CN (0.5 mL), 60±1 °C, monitored by following changes of enamine signals by ^{1}H-NMR at 23 °C, data were collected as the average of two individual experiments. [b] Calculated by nonlinear regression analysis towards standard reaction model (see Supporting Information). [c] $k_f/k_{f,uncat}$, $k_{f,uncat}$ were the corresponding rates in Table 1. [d] Ratio of [Enamine exchanged]/[Enamine original] at equilibrium. [e] Ratio of [Enamine exchanged]^2/(1−[Enamine exchanged]^2) at equilibrium.

Conclusions

In summary, coupled configurational and constitutional dynamics based on enamine molecular switches have been systematically studied. The enamine switches could be readily obtained through a one-step condensation of primary amines with the stator compounds. In order to achieve complete acid/base-dependent switching around the enamine double bond, pH-responsive moieties, such as 2-pyridyl and 2-quinolinyl units, were required on the stator part, also providing enamine stability through IMHB effects. Having 2-pyridyl as the stator, the switching efficiency and the stability of the switches were found to be correlated. By extending the stator π-system in the 2-quinolinyl derivative, a higher *E*-isomeric equilibrium ratio was obtained under neutral conditions, thus indicating a means to obtain quantitative forward/backward isomerization processes. Dynamic constitutional systems can be easily generated from enamines undergoing exchange with various amines. Generally, considerably higher exchange rates were observed with amines containing ester groups, indicating potential stabilization of the **TS** trough IMHB by the ester groups. Various acids, particularly Bi^{III}, were found to efficiently catalyze the dynamic processes, especially in cases exhibiting slow, uncatalyzed kinetics. The addition of excess amounts of TFA led to inhibition of the dynamic exchange in certain cases. Under basic conditions, in contrast to imines, the enamines studied exhibited high stability and no exchange with primary amines. This potentiates orthogonal switching and exchange, where dynamic systems of varied configuration states can be accessed through orthogonal reactions. This novel type of double dynamic system, operating under both configurational and constitutional regimes, enables a range of potential applications. We thus envision that the switches, for example, can be exploited as elements at surfaces and within materials, with the potential for applications in drug delivery and/or nanotechnology. Besides, the properties of dynamic materials can be controlled by regulating the complexity of the dynamic systems.

Acknowledgements

This study was in part supported by the Swedish Research Council. Y.R. thanks the China Scholarship Council for a special award.

Conflict of interest

The authors declare no conflict of interest.

Keywords: constitutional · dynamic · enamine · responsive · switch

[1] G. Wittig, H. Blumenthal, *Ber. Dtsch. Chem. Ges.* **1927**, *60*, 1085 – 1094.
[2] a) Y. Q. Zou, F. M. Hormann, T. Bach, *Chem. Soc. Rev.* **2018**, *47*, 278 – 290; b) V. A. Bakulev, T. Beryozkina, J. Thomas, W. Dehaen, *Eur. J. Org. Chem.* **2018**, 262 – 294; c) S. Wang, *Isr. J. Chem.* **2018**, *58*, 557 – 567; d) H. M. Gaber, M. C. Bagley, Z. A. Muhammad, S. M. Gomha, *RSC Adv.* **2017**, *7*, 14562 – 14610; e) D. V. Dar'in, P. S. Lobanov, *Russ. Chem. Rev.* **2015**, *84*, 601 – 633; f) A. Erkkilä, I. Majander, P. M. Pihko, *Chem. Rev.* **2007**, *107*, 5416 – 5470; g) S. Mukherjee, J. W. Yang, S. Hoffmann, B. List, *Chem. Rev.* **2007**, *107*, 5471 – 5569; h) W. Notz, F. Tanaka, C. F. Barbas 3rd, *Acc. Chem. Res.* **2004**, *37*, 580 – 591.
[3] a) Y. Ren, P. H. Svensson, O. Ramström, *Angew. Chem. Int. Ed.* **2018**, *57*, 6256 – 6260; *Angew. Chem.* **2018**, *130*, 6364 – 6368; b) Y. Zhang, S. Xie, M. Yan, O. Ramström, *Chem. Eur. J.* **2017**, *23*, 11908 – 11912.
[4] a) Y. Zhang, Y. Qi, S. Ulrich, M. Barboiu, O. Ramström, *Mater. Chem. Front.* **2020**, *4*, 489 – 506; b) P. Frei, R. Hevey, B. Ernst, *Chem. Eur. J.* **2019**, *25*, 60 – 73; c) Y. Zhang, Y. Zhang, O. Ramström, *Cat. Rev. Sci. Eng.* **2020**, *62*, 66 – 95; d) A. G. Orrillo, A. M. Escalante, M. Martinez-Amezaga, I. Cabezudo, R. L. E. Furlan, *Chem. Eur. J.* **2019**, *25*, 1118 – 1127; e) W. Zhang, Y. Jin, *Dynamic Covalent Chemistry: Principles, Reactions, and Applications*, Wiley, **2017**; f) O. Š. Miljanić, *Chem* **2017**, *2*, 502 – 524; g) T. Kosikova, D. Philp, *Chem. Soc. Rev.* **2017**, *46*, 7274 – 7305; h) I. Azcune, I. Odriozola, *Eur. Polym. J.* **2016**, *84*, 147 – 160; i) R.-C. Brachvogel, M. von Delius, *Eur. J. Org. Chem.* **2016**, 3662 – 3670; j) Y. Zhang, M. Barboiu, *Chem. Rev.* **2016**, *116*, 809 – 834; k) J. M. Lehn, *Angew. Chem. Int. Ed.* **2015**, *54*, 3276 – 3289; *Angew. Chem.* **2015**, *127*, 3326 – 3340; l) A. Herrmann, *Chem. Soc. Rev.* **2014**, *43*, 1899 – 1933; m) L. Hu, F. Schaufelberger, B. J. J. Timmer, M. A. Flos, O. Ramström in *Kirk-Othmer Encyclopedia of Chemical Technology*, Wiley, **2014**, pp. 1 – 25; n) M. C. Misuraca, E. Moulin, Y. Ruff, N. Giuseppone, *New J. Chem.* **2014**, *38*, 3336 – 3349; o) A. Wilson, G. Gasparini, S. Matile, *Chem. Soc. Rev.* **2014**, *43*, 1948 – 1962; p) Y. Jin, C. Yu, R. J. Denman, W. Zhang, *Chem. Soc. Rev.* **2013**, *42*, 6634 – 6654; q) R. A. Hunt, S. Otto, *Chem. Commun.* **2011**, *47*, 847 – 858; r) G. Gasparini, M. Dal Molin, L. J. Prins, *Eur. J. Org. Chem.* **2010**, 2429 – 2440.
[5] a) H. Zou, Y. Hai, H. Ye, L. You, *J. Am. Chem. Soc.* **2019**, *141*, 16344 – 16353; b) S. Kassem, A. T. L. Lee, D. A. Leigh, V. Marcos, L. I. Palmer, S. Pisano, *Nature* **2017**, *549*, 374 – 378; c) S. Kassem, A. T. Lee, D. A. Leigh, A. Markevicius, J. Solà, *Nat. Chem.* **2016**, *8*, 138 – 143; d) P. Kovaříček, J.-M. M. Lehn, *J. Am. Chem. Soc.* **2012**, *134*, 9446 – 9455; e) M. von Delius, D. A. Leigh, *Chem. Soc. Rev.* **2011**, *40*, 3656 – 3676.
[6] M. N. Chaur, D. Collado, J. M. Lehn, *Chem. Eur. J.* **2011**, *17*, 248 – 258.
[7] P. L. Jackson-Ayotunde, M. S. Alexander, I. O. Edafiogho, K. R. Scott, in *Applications of NMR Spectroscopy: Volume 3* (Ed.: M. I. Choudhary), Bentham Science Publishers, **2015**, pp. 150 – 178.
[8] a) K. T. Mahmudov, A. J. Pombeiro, *Chem. Eur. J.* **2016**, *22*, 16356 – 16398; b) P. Gilli, L. Pretto, V. Bertolasi, G. Gilli, *Acc. Chem. Res.* **2009**, *42*, 33 – 44; c) V. Bertolasi, L. Pretto, V. Ferretti, P. Gilli, G. Gilli, *Acta Crystallogr. Sect. B* **2006**, *62*, 1112 – 1120; d) G. Gilli, P. Gilli, *J. Mol. Struct.* **2000**, *552*, 1 – 15.
[9] N. Abeyrathna, Y. Liao, *J. Am. Chem. Soc.* **2015**, *137*, 11282 – 11284.
[10] L. Kozerski, B. Kwiecień, R. Kawęcki, Z. Urbańczyk-Lipkowska, W. Bocian, E. Bednarek, J. Sitkowski, J. Maurin, L. Pazderski, P. E. Hansen, *New J. Chem.* **2004**, *28*, 1562 – 1567.
[11] a) J. E. Johnson, N. M. Morales, A. M. Gorczyca, D. D. Dolliver, M. A. McAllister, *J. Org. Chem.* **2001**, *66*, 7979 – 7985; b) I. Yavari, A. Shaabani, H. Soliemani, F. Nourmohammadian, H. R. Bijanzadeh, *Magn. Reson. Chem.* **1996**, *34*, 1003 – 1006; c) A. R. E. Carey, G. Fukata, R. A. M. O'Ferrall, M. G. Murphy, *J. Chem. Soc. Perkin Trans. 2* **1985**, 1711 – 1722; d) V. I. Bakhmutov, *Bull. Magn. Reson.* **1984**, *6*, 142 – 153.
[12] Gaussian 09, Rev.D.01. M. J. Frisch, G. W. Trucks, H. B. Schlegel, G. E. Scuseria, M. A. Robb, J. R. Cheeseman, G. Scalmani, V. Barone, B. Mennucci, G. A. Petersson, H. Nakatsuji, M. Caricato, X. Li, H. P. Hratchian, A. F. Izmaylov, J. Bloino, G. Zheng, J. L. Sonnenberg, M. Hada, M. Ehara, K. Toyota, R. Fukuda, J. Hasegawa, M. Ishida, T. Nakajima, Y. Honda, O. Kitao, H. Nakai, T. Vreven, J. A. Montgomery, J. E. Peralta, F. Ogliaro, M. Bearpark, J. J. Heyd, E. Brothers, K. N. Kudin, V. N. Staroverov, R. Kobayashi, J. Normand, K. Raghavachari, A. Rendell, J. C. Burant, S. S. Iyengar, J. Tomasi, M. Cossi, N. Rega, J. M. Millam, M. Klene, J. E. Knox, J. B. Cross, V. Bakken, C. Adamo, J. Jaramillo, R. Gomperts, R. E. Stratmann, O. Yazyev, A. J. Austin, R. Cammi, C. Pomelli, J. W. Ochterski, R. L. Martin, K. Morokuma, V. G. Zakrzewski, G. A. Voth, P. Salvador, J. J. Dannenberg, S. Dapprich, A. D. Daniels, Ö. Farkas, J. B. Foresman, J. V. Ortiz, J. Cioslowski, D. J. Fox, Wallingford CT, **2009**.
[13] A. D. Becke, *J. Chem. Phys.* **1993**, *98*, 5648 – 5652.
[14] M. M. Francl, W. J. Pietro, W. J. Hehre, J. S. Binkley, M. S. Gordon, D. J. DeFrees, J. A. Pople, *J. Chem. Phys.* **1982**, *77*, 3654 – 3665.
[15] S. M. Landge, E. Tkatchouk, D. Benitez, D. A. Lanfranchi, M. Elhabiri, W. A. Goddard 3rd, I. Aprahamian, *J. Am. Chem. Soc.* **2011**, *133*, 9812 – 9823.
[16] D. D. Perrin, *Dissociation Constants of Organic Bases in Aqueous Solution*, Butterworths, London, **1965**.
[17] N. Giuseppone, J. L. Schmitt, E. Schwartz, J. M. Lehn, *J. Am. Chem. Soc.* **2005**, *127*, 5528 – 5539.
[18] F. Schaufelberger, B. J. J. Timmer, O. Ramström in *Dynamic Covalent Chemistry*, Wiley, **2017**, pp. 1 – 30.
[19] a) M. F. Carvalho, M. J. Ferreira, A. S. Knittel, C. Oliveira Mda, J. Costa Pessoa, R. Herrmann, G. Wagner, *Beilstein J. Org. Chem.* **2016**, *12*, 732 – 744; b) G. Gasparini, M. Martin, L. J. Prins, P. Scrimin, *Chem. Commun.* **2007**, 1340 – 1342; c) C. F. Rodriquez, A. Cunje, T. Shoeib, I. K. Chu, A. C. Hopkinson, K. W. M. Siu, *J. Am. Chem. Soc.* **2001**, *123*, 3006 – 3012; d) R. B. Sharma, A. T. Blades, P. Kebarle, *J. Am. Chem. Soc.* **1984**, *106*, 510 – 516; e) J. Toullec, R. Razafindralambo, *J. Org. Chem.* **1987**, *52*, 1646 – 1647.
[20] M. Ciaccia, R. Cacciapaglia, P. Mencarelli, L. Mandolini, S. Di Stefano, *Chem. Sci.* **2013**, *4*, 2253.
[21] P. F. McGarry, S. Jockusch, Y. Fujiwara, N. A. Kaprinidis, N. J. Turro, *J. Phys. Chem. A* **1997**, *101*, 764 – 767.
[22] a) F. Schaufelberger, K. Seigel, O. Ramström, *Chem. Eur. J.* **2020**, https://doi.org/10.1002/chem.202001666; b) H. Jędrzejewska, M. Wierzbicki, P. Cmoch, K. Rissanen, A. Szumna, *Angew. Chem. Int. Ed.* **2014**, *53*, 13760 – 13764; *Angew. Chem.* **2014**, *126*, 13980 – 13984; c) A. Sanchez-Sanchez, D. A. Fulton, J. A. Pomposo, *Chem. Commun.* **2014**, *50*, 1871 – 1874; d) A. Paul, S. Ladame, *Org. Lett.* **2009**, *11*, 4894 – 4897.
[23] M. Ciaccia, S. Di Stefano, *Org. Biomol. Chem.* **2015**, *13*, 646 – 654.
[24] a) S. Kulchat, M. N. Chaur, J. M. Lehn, *Chem. Eur. J.* **2017**, *23*, 11108 – 11118; b) D. Schultz, J. R. Nitschke, *J. Am. Chem. Soc.* **2006**, *128*, 9887 – 9892.

Manuscript received: July 25, 2020
Accepted manuscript online: October 12, 2020
Version of record online: November 17, 2020